Acta Biomaterialia 44 (2016) 31–40

Contents lists available at ScienceDirect

Acta Biomaterialia

journal homepage: www.elsevier.com/locate/actabiomat

Full length article

Enhanced protective role in materials with gradient structural orientations: Lessons from Nature

Zengqian Liu [a,b], Yankun Zhu [b], Da Jiao [b], Zhaoyong Weng [b], Zhefeng Zhang [b,*], Robert O. Ritchie [a,*]

[a] Department of Materials Science and Engineering, University of California, Berkeley, CA 94720, USA
[b] Shenyang National Laboratory for Materials Science, Institute of Metal Research, Chinese Academy of Sciences, Shenyang 110016, China

ARTICLE INFO

Article history:
Received 21 May 2016
Received in revised form 8 July 2016
Accepted 4 August 2016
Available online 5 August 2016

Keywords:
Gradient
Biological materials
Bioinspired design
Structural orientation
Functionally graded materials

ABSTRACT

Living organisms are adept at resisting contact deformation and damage by assembling protective surfaces with spatially varied mechanical properties, *i.e.*, by creating functionally graded materials. Such gradients, together with multiple length-scale hierarchical structures, represent the two prime characteristics of many biological materials to be translated into engineering design. Here, we examine one design motif from a variety of biological tissues and materials where site-specific mechanical properties are generated for enhanced protection by adopting gradients in structural orientation over multiple length-scales, without manipulation of composition or microstructural dimension. Quantitative correlations are established between the structural orientations and local mechanical properties, such as stiffness, strength and fracture resistance; based on such gradients, the underlying mechanisms for the enhanced protective role of these materials are clarified. Theoretical analysis is presented and corroborated through numerical simulations of the indentation behavior of composites with distinct orientations. The design strategy of such bioinspired gradients is outlined in terms of the geometry of constituents. This study may offer a feasible approach towards generating functionally graded mechanical properties in synthetic materials for improved contact damage resistance.

Statement of Significance

Living organisms are adept at resisting contact damage by assembling protective surfaces with spatially varied mechanical properties, *i.e.*, by creating functionally-graded materials. Such gradients, together with multiple length-scale hierarchical structures, represent the prime characteristics of many biological materials. Here, we examine one design motif from a variety of biological tissues where site-specific mechanical properties are generated for enhanced protection by adopting gradients in structural orientation at multiple length-scales, without changes in composition or microstructural dimension. The design strategy of such bioinspired gradients is outlined in terms of the geometry of constituents. This study may offer a feasible approach towards generating functionally-graded mechanical properties in synthetic materials for improved damage resistance.

Published by Elsevier Ltd on behalf of Acta Materialia Inc.

1. Introduction

The increasingly stringent requirement for the enhanced performance of materials has stimulated the concept of functionally graded materials (FGMs) which encompass spatial gradients of composition or/and structural characteristics in continuous or fine discrete manner. Compared to the traditional materials that are usually homogeneous or possess abrupt changes of composition/structure, the overall properties of FGMs benefit from their gradients in a range of aspects [1–4]. A prime example is the graded metal-ceramic composites designed for thermal barrier applications [1,2]. The thermal stress and resultant damage can be effectively mitigated by introducing a smooth compositional transition over the volume by manipulating the spatial dispersions of constituents [4,5]. Another advantage of FGMs is their enhanced resistance to contact deformation and damage [6,7]. A customary motif is to utilize relatively harder materials, generally at a surface that experiences a high stress, to resist wear and/or penetration, and to employ relatively tougher materials, generally at the sub-surface region, to accommodate deformation, dissipate mechanical energy and arrest the propagation of cracks.

* Corresponding authors.
E-mail addresses: zhfzhang@imr.ac.cn (Z. Zhang), roritchie@lbl.gov (R.O. Ritchie).

http://dx.doi.org/10.1016/j.actbio.2016.08.005
1742-7061/Published by Elsevier Ltd on behalf of Acta Materialia Inc.

The processing and properties of FGMs have attracted considerable research interest over the past two decades [1–4,6]. A common strategy that has been most frequently adopted is to control the spatial distribution of compositions or constituents [3]. For example, a ceramic-glass FGM with improved indentation toughness can be generated by infiltrating an oxynitride glass into a silicon nitride matrix [7]. Alternatively, the characteristic dimension of the structural units can be manipulated; a prime example is the gradient nano-grained metals fabricated by surface mechanical grinding treatment [8]. Additionally, elastic gradients can be created in laminated composites via a stepwise variation of the in-plane alignment of fibers between adjacent laminates [9].

Although the idea of FGMs is relatively new in the engineering field (the concept was first proposed in 1980s in Japan [1,2]), the design principle has long been utilized in Nature by optimizing the performance of numerous biological materials [10–19]. For example, bamboo, as a naturally-occurring FGM, features a composite structure reinforced by vascular bundles that comprise mainly cellulose fibers aligned along the long axis of stem [12]. These bundles are distributed in a graded fashion with decreasing density from the outermost periphery inwards, leading to graded mechanical properties that endow the bamboo with enhanced flexural rigidity [13]. An important class of natural FGMs are biological armors, such as fish scales [14–16], mollusk shells [17,18] and alligator osteoderms [19], wherein distinct layers are usually assembled to generate site-specific properties for enhanced protection to penetration, *e.g.*, caused by the biting attack from predators. Although it is doubtful whether the primitive idea for early graded materials, such as the blades of Samurai or ancient Chinese bronze swords [20], originated from Nature, biological materials may offer fruitful inspiration for the development of such high-performance synthetic FGMs.

Here we extract one salient natural design motif of FGMs used to enhance offense and/or defense against predators from a multitude of biological materials and components where functionally graded mechanical properties can be achieved by tuning the structural orientations. Variations in local mechanical properties with structural orientation, including stiffness, strength and fracture resistance, are quantitatively elucidated and the mechanisms for improved protection clarified and further visualized by numerical simulation.

2. Gradient structural orientations in Nature

Biological materials are generally composites comprising relatively hard and soft components and have evolved complex hierarchical architectures that have been ingeniously optimized from nano to macro length-scales for their specific functions [21–24]. This is particularly true for tissues or materials serving as offensive weapons and/or defensive armors; both are vital for most living organisms. Such biological design has developed through the long-period "evolutionary arms race", in particular using continuously varying structural orientations, with mechanical efficiency as the central concern [15,25]. Notable examples of macro tissues in this type are the horns of yak and antelope [26], tusks of wild boar, walrus and elephant [27], claws of lobster and crab [28,29], scorpion stingers [30], spider fangs [31,32], and worm jaws [33,34], as shown in Fig. 1. The long axes of these tissues change gradually towards their apexes to approach the direction of external force experienced therein (the external force is generally nearly tangent to the centerline [30–32]), so that the overall orientation continuously deviates from the external force with increasing distance from the loading site.

In addition to the macroscopic geometry, a number of biological materials possess graded structural orientations at the micro/nano length-scales. For example, in nacreous shell materials, the first-order constituent layers along the thickness are gradually tilted from being parallel to the surface in the interior to being oblique

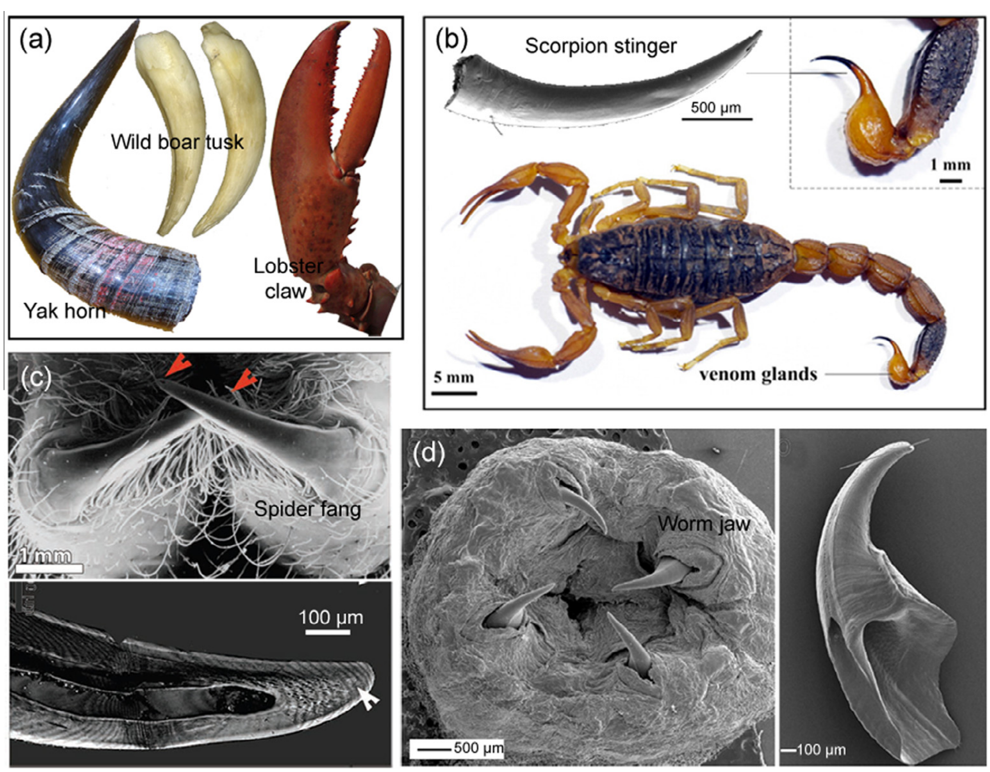

Fig. 1. Continuously curving shapes in representative biological tissues of yak horn, wild boar tooth, lobster claw (a), scorpion stinger (b), spider fang (c), and worm jaw (d). (b-d) are adapted with permission from Refs. [30,31,34].

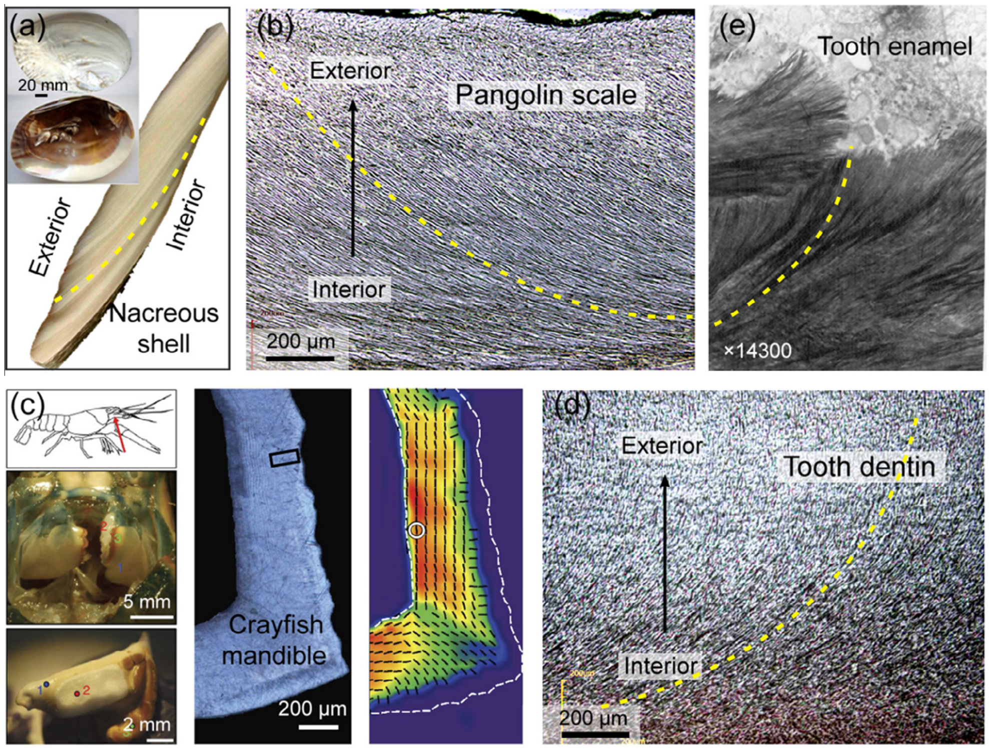

Fig. 2. Continuously varying structural orientations in typical natural materials of nacreous shell (a), pangolin scale (b), crayfish mandible (c), tooth dentin (d), and tooth enamel (e). The orientations of chitin fibers in crayfish mandible are denoted by black lines. The structural orientations of other tissues are indicated by dashed curves. (c) and (e) are adapted with permission from Refs. [37,41].

with the surface in the exterior (Fig. 2a). This is analogous to the macro tissues discussed above as both display increasing misorientation between the structure and the externally applied forces with the distance from loading site (for shells, the external force is generally caused by predator attack, *e.g.*, biting, which is commonly applied normal to the surface). Many biological materials exhibit similar structural variations at the micrometer level, among which pangolin scale and crayfish mandible are prime examples [35–37], as shown in Fig. 2b and c. The constituents, *i.e.*, keratin laminates in pangolin scale and chitin fibers in crayfish mandible, are aligned almost along the inner surface of tissue in the interior and continuously tilted towards the outer surface. A similar structure also exists in the mammalian tooth dentin wherein the dentin tubules are arranged in a radial form from the pulp chamber to the dentin-enamel junction (Fig. 2d) [38,39]. Moreover, such features are common at the sub-micrometer to nano-scale levels in Nature as exemplified by the outstretching alignment of hydroxyapatite fibers within the mineral prisms in tooth enamel (Fig. 2e) [40–43]. The widespread application of varying structural orientations at multiple length-scales represents a salient design motif in biological materials where the principle of gradually deviating the orientation of the primary structural feature from the direction of the external force is employed to enhance function and mechanical performance.

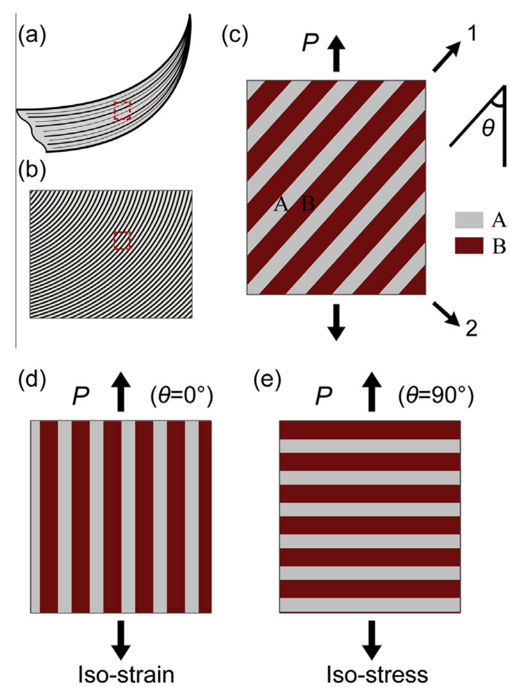

Fig. 3. Schematic illustrations of the varying structural orientations in biological tissues (a) and materials (b) and an elementary block extracted from them where the constituents, principal orientations and structural orientation angle are indicated (c). Schematic illustrations of the iso-strain (d) and iso-stress (e) conditions of constituents in the composite when loaded parallel and orthogonal to the long axis of laminates, respectively.

3. Functionally graded mechanical properties

To explore the mechanical rationale for the natural architectures described above, an elementary structural unit, where the orientation change can be ignored, is extracted from the biological tissues and/or materials, as illustrated in Fig. 3a-c. Here we consider a composite material where the relatively soft and hard components are alternately assembled in two-dimensional coordinates. The soft phase *A* acts as the compliant organic matter or weak interface, while the hard phase *B* mainly offers stiffness and strength generally in the form of minerals or sub-structural constituents in biological materials [21–24,44,45]. As such, this model is capable of describing a wide range of biological materials encompassing laminated (*e.g.*, pangolin scale [35,36]), tubular (*e.g.*, tooth dentin [38,39]), and fibrous structures (*e.g.*, hair [35,46]), *etc.*

For simplification, the individual constituents are treated as homogeneous and isotropic without taking their internal complexities into account. V_A and V_B denote the volume fractions of corresponding phases with $V_A + V_B = 1$. The orientations that are parallel and orthogonal to the long axis of constituents are designated as 1 and 2, respectively. The misorientation between the structure and external force P is defined as the orientation angle θ, such that θ equals to 0° and 90°, respectively, for loading along the orientations 1 and 2. Below we quantitatively elaborate how materials can derive functional gradients in three important mechanical properties, *i.e.*, stiffness, strength and fracture resistance, for enhanced protection by tuning the orientations of their structural features.

3.1. Stiffness

Stiffness, as a measure of material's resistance to elastic deformation, relies principally on the Young's modulus. As illustrated in Fig. 3d and e, the constituents of composites sustain equivalent strain and stress, respectively, when loaded elastically along the orientations 1 and 2. The apparent Young's moduli of composites in these conditions can be simply described according to the rule-of-mixtures under iso-strain (Voigt) and iso-stress (Reuss) states, respectively, following $E_1 = E_A V_A + E_B V_B$ and $\frac{1}{E_2} = \frac{V_A}{E_A} + \frac{V_B}{E_B}$, where E_A and E_B are the Young's moduli of A and B phases and the subscripts 1 and 2 represent the corresponding orientations [47,48].

Accordingly, the apparent Young's modulus, E_P, along an arbitrary loading direction with orientation angle θ can be obtained following the laminate theory according to:

$$\frac{1}{E_P} = \frac{\cos^4\theta}{E_1} + \left(\frac{1}{G_{12}} - \frac{2\nu_{12}}{E_1}\right)\sin^2\theta\cos^2\theta + \frac{\sin^4\theta}{E_2}, \tag{1}$$

where G_{12} and ν_{12} are the shear modulus and Poisson's ratio of composite in the 1–2 plane, respectively [47,49,50]. In the present case, G_{12} and ν_{12} can be obtained from:

$$\frac{1}{G_{12}} = \frac{V_A}{G_A} + \frac{V_B}{G_B}, \tag{2}$$

and

$$\nu_{12} = \nu_A V_A + \nu_B V_B, \tag{3}$$

respectively, where G_A, G_B and ν_A, ν_B denote the shear moduli and Poisson's ratios of the corresponding phases [47].

Additionally, the elastic constants are intrinsically related by $G_A = \frac{E_A}{2(1+\nu_A)}$ and $G_B = \frac{E_B}{2(1+\nu_B)}$ within the individual constituents [51]. We assume that there is an identical Poisson's ratio between the two phases, *i.e.*, $\nu_A = \nu_B = \nu$, which approximates to 0.3 in a variety of biological materials [24,48], and a constant ratio between their Young's moduli, *i.e.*, $k = E_B/E_A > 1$. As such, the apparent Young's modulus of the composite normalized by that of the soft phase can be obtained by incorporating the involved parameters into Eq. (1) as:

$$\frac{E_P}{E_A} = \left\{\frac{\cos^4\theta}{V_A + k - kV_A} + \left[\frac{2(1+\nu)(kV_A + 1 - V_A)}{k} - \frac{2\nu}{V_A + k - kV_A}\right] \times \sin^2\theta\cos^2\theta + \frac{kV_A + 1 - V_A}{k}\sin^4\theta\right\}^{-1} \tag{4}$$

The variation in the ratio E_P/E_A, as a function of the volume fraction of the soft constituent V_A and orientation angle θ (at constant k), is shown in Fig. 4a; the orientation effects are further specified in Fig. 4b for different combinations of k and V_A. The Young's modulus can be seen to decrease monotonically with the increase in orientation angle, specifically in a steeper fashion at the lower misorientation range. By this means, the naturally varying structural orientations result in an elastic gradient in which the material becomes stiffer to resist deformation towards the surface yet more compliant to accommodate the stress towards the interior.

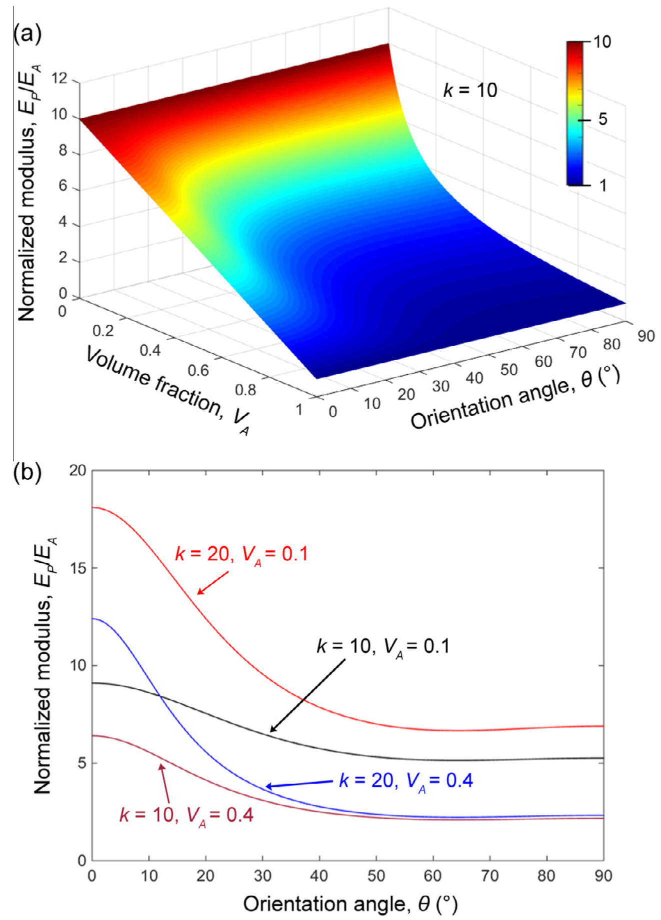

Fig. 4. (a) Dependences of normalized Young's modulus of the composite, E_P/E_A, on the volume fraction of the soft phase V_A and orientation angle θ at a constant k of 10. (b) Variations in E_P/E_A as a function of θ for representative cases of different k and V_A.

3.2. Strength

Strength, representing the material's resistance to unrecoverable (strictly inelastic) deformation and damage, is closely associated with the detailed failure modes which originate in an orthotropic composite depending on the loading state and orientation, as illustrated by the insets in Fig. 5. Under uniaxial tension, the longitudinal strength of the composite along the orientation 1, σ_1, generally corresponds to the failure of the hard phase, *e.g.*, reinforced fibers, so that σ_1 relies to a large extent on the strength of hard phase, σ_B; conversely, the transverse strength, σ_2, is determined by the strength of the soft phase, σ_A [47,49]. The strength anisotropy, *i.e.*, the ratio between the strengths corresponding to orientations 1 and 2, can thus be described as $m = \sigma_1/\sigma_2 = \sigma_1/\sigma_A$, which is invariably larger than unity. Under a state of compressive loading, the transverse strength σ_2 can be presumed to remain constant as it is still dominated by the failure

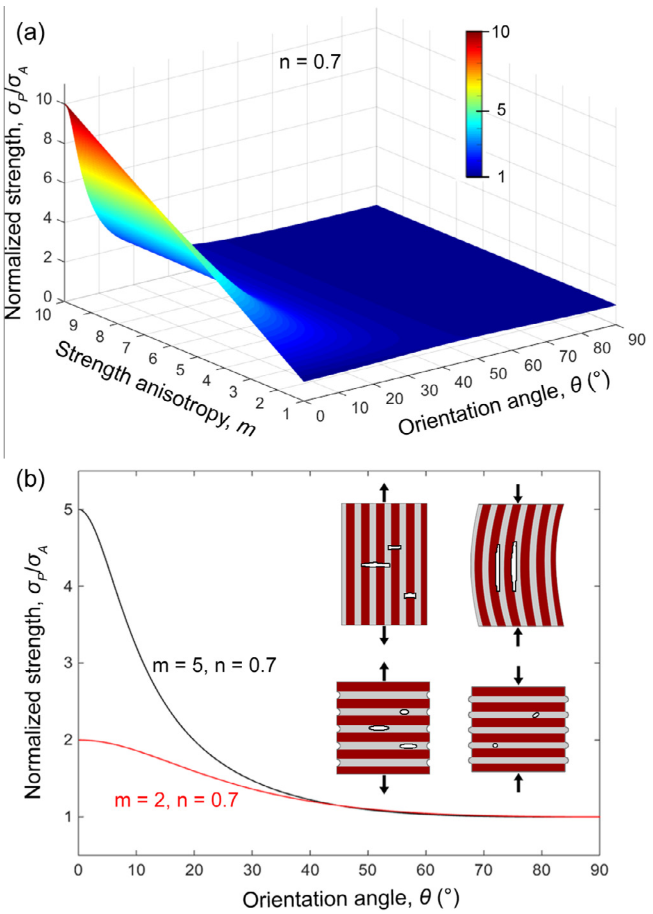

Fig. 5. (a) Variations in the normalized strength of composite σ_P/σ_A as a function of the strength anisotropy m and orientation angle θ at a constant n of 0.7. (b) Dependences of σ_P/σ_A on θ for different m values of 5 and 2, which represent the cases of uniaxial tension and compression, respectively. Representative failure modes of the composite along the longitudinal and transverse directions under uniaxial tension and compression are illustrated in the insets of (b).

of the soft phase (without considering the tension-compression strength asymmetry of the individual constituent). Nonetheless, premature failure may occur in the composite as a result of mechanical instability, *e.g.*, compressive buckling, along the longitudinal orientation [47,48,51], thus diminishing σ_1. Consequently, the effect of stress state on the principal strengths can be depicted using the parameter m, with m larger for tension than for compression.

According to the Tsai-Hill failure criterion for orthotropic materials [47,49–52], the off-axial strength of the composite, σ_P, at an arbitrary orientation angle θ can be obtained by the following relation:

$$\frac{1}{\sigma_p^2} = \frac{\cos^4\theta}{\sigma_1^2} + \left(\frac{1}{\tau_{12}^2} - \frac{1}{\sigma_1^2}\right)\sin^2\theta\cos^2\theta + \frac{\sin^4\theta}{\sigma_2^2}, \tag{5}$$

where τ_{12} denotes the shear strength in 1–2 plane that is presumed to be primarily governed by the shear failure of the soft phase. We define a parameter n as the ratio between τ_{12} and σ_2, *i.e.*, $n = \tau_{12}/\sigma_2 = \tau_{12}/\sigma_A$, which reflects the inherent shearing propensity relative to normal failure of the composite along its weak orientation. By incorporating the parameters m and n into Eq. (5), the apparent strength of the composite normalized by that of the soft phase, σ_P/σ_A, can be expressed as:

$$\frac{\sigma_P}{\sigma_A} = \left[\frac{\cos^4\theta}{m^2} + \left(\frac{m^2-n^2}{m^2n^2}\right)\sin^2\theta\cos^2\theta + \sin^4\theta\right]^{-1/2}. \tag{6}$$

Fig. 5a shows the dependence of σ_P/σ_A on the strength anisotropy m and orientation angle θ for a constant n of 0.7. σ_P/σ_A decreases monotonically with the decrease in m and/or increase in θ. Specific cases for uniaxial tension and compression are represented by adopting relatively high and low values of m (m is chosen as 5 and 2 for tension and compression, respectively), as shown in Fig. 5b. Invariably, the strength of the composite displays a similar trend as the stiffness with the misorientation between the structure and external force. As such, by utilizing the varying structural orientations, biological materials derive an enhanced resistance to the onset of damage from higher strength towards the surface, and at the same time, redistribute the stress and dissipate more mechanical energy towards the interior by allowing easier plastic deformation.

3.3. Fracture resistance

Fracture toughness, reflecting the material's resistance to the initiation and growth of cracks, may arise from a variety of toughening mechanisms that are either intrinsic or extrinsic [23,53,54]. Intrinsic toughening mechanisms are active at small length-scales ahead of the crack tip and normally associated with

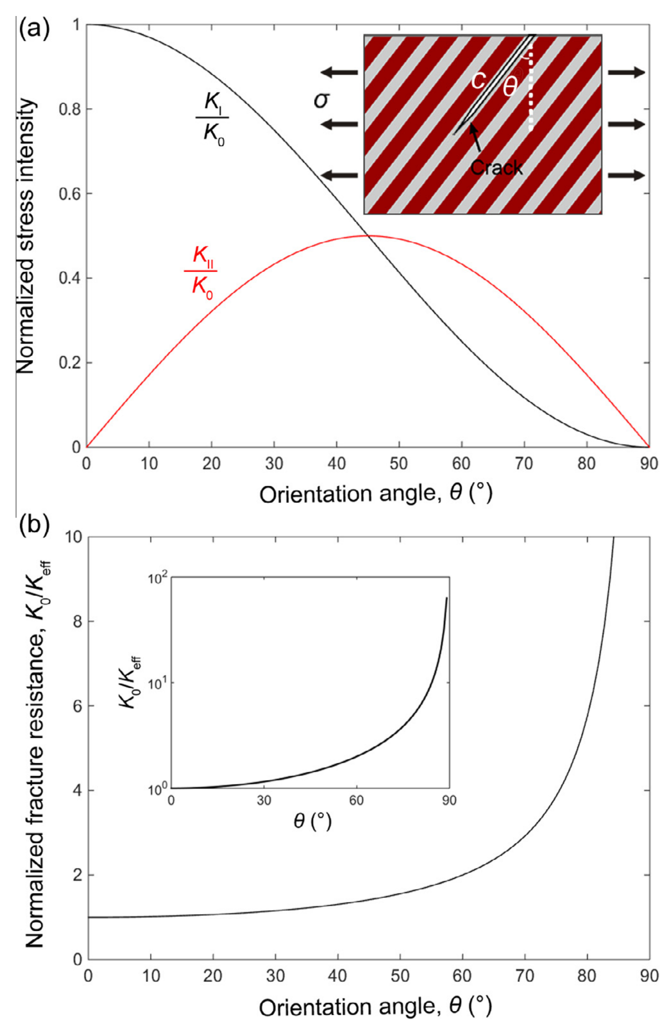

Fig. 6. (a) Variations of the mode I and mode II stress intensities of a deflected crack normalized by that of an idealized pure mode I crack, K_I/K_0 and K_{II}/K_0, as a function of orientation angle θ in the composite. The inward growth of the main crack along the structural features of the composite subjected to in-plane tension is illustrated in the inset. (b) Dependence of normalized fracture resistance of the composite represented using the reciprocal of effective stress intensity K_{eff} normalized by K_0, *i.e.*, K_0/K_{eff}, on θ. The inset presents such a relationship in logarithmic form.

the inherent plasticity of materials. At coarser length-scales, toughening may be generated from a series of extrinsic mechanisms that act to shield the crack tip from applied stress. In particular, such mechanisms are facilitated in many biological materials by their intricate structure as major sources of toughness. A basic strategy of extrinsic toughening, which has been identified in a variety of materials, *e.g.*, bone [23,54–56], is to deflect the crack away from its preferred path with the maximum driving force. As such, the crack propagation necessitates higher mechanical stress or energy, thus offering improved toughness. In the present case, the intrinsic toughening mechanisms of the composite are not influenced as the constituents and their properties are unchanged. Nevertheless, the varying structural orientations can lead to continuous crack deflection along them, thereby enabling significant extrinsic toughening.

To imitate the actual situation in biological armors, we examine the inward propagation of a crack with length of c in an elementary composite subjected to an in-plane tensile stress σ, as illustrated by the inset in Fig. 6a. Here the crack is assumed to be trapped within the weak phase without considering its trans-lamellar growth. Accordingly, the inclination angle between the crack path and the thickness direction equals to the orientation angle θ of the composite. The crack tip is exposed to a mixed-mode loading state of tension and shear, where the driving forces for crack growth can be described using the mode I and mode II stress intensities, respectively, as:

$$K_{\mathrm{I}} = \psi\sigma\sqrt{\pi c}\cos^2\theta, \tag{7}$$

and

$$K_{\mathrm{II}} = \psi\sigma\sqrt{\pi c}\sin\theta\cos\theta, \tag{8}$$

where ψ is the dimensionless geometry parameter [57–59]. The effect of structural orientation can be described by normalizing the stress intensities using that of an idealized crack with the same length subjected to pure tension, *i.e.*, $K_0 = \psi\sigma\sqrt{\pi c}$, as:

$$\frac{K_{\mathrm{I}}}{K_0} = \cos^2\theta, \tag{9}$$

and

$$\frac{K_{\mathrm{II}}}{K_0} = \sin\theta\cos\theta. \tag{10}$$

As shown in Fig. 6a, K_{I}/K_0 decreases monotonically with increasing orientation angle θ; while K_{II}/K_0 is highest at $\theta = 45^\circ$ and decreases towards both sides.

The effective stress intensity K_{eff} for the inclined crack can be obtained by combining the mode I and mode II components in terms of the strain energy release rate [57–63]:

$$K_{eff} = \sqrt{K_{\mathrm{I}}^2 + K_{\mathrm{II}}^2} = \psi\sigma\sqrt{\pi c}\cos\theta. \tag{11}$$

Such a relation is capable of describing the effective driving force for crack propagation under mixed-mode loading conditions and has been widely applied in a range of materials, in particular biological materials, such as human cortical bone [62] and tooth dentin [63]. Because the intrinsic toughening mechanisms of the composite remain constant, the difficulty of crack propagation can be represented using the reciprocal of its driving force, *i.e.*, lower driving force signifies higher potency of crack-tip shielding. Accordingly, the fracture resistance of the composite normalized by that of the idealized crack can be described as:

$$\frac{K_0}{K_{eff}} = \frac{1}{\cos\theta}. \tag{12}$$

K_0/K_{eff} increases monotonically as the crack deflects with increasing θ along the structural feature (Fig. 6b). As a result, the extrinsic toughening effect is continuously enhanced as the crack propagates from the surface towards the interior, leading to increased crack-growth resistance. Of note here is that elastic and plastic deformation is more prone to occur in materials with increasing thickness owing to the decreases in local stiffness and strength. Such a combination of graded mechanical properties, with opposite varying trends of stiffness/strength and toughness which imply the intrinsic conflicts between them [64], markedly diminishes the mechanical damage in the material for enhanced protection.

4. Simulation of indentation behavior

To visualize the above analysis, the mechanical behavior under indentation loading of three hybrid composites with distinct architectures, *i.e.*, unidirectionally axial and orthotropic laminates and a composite with varying structural orientation, was numerically simulated using finite element analysis (FEA, ANSYS 15.0). Two-dimensional volumes with length of 1.2 mm and height of 0.8 mm were adopted in the simulation in which the lateral and bottom boundaries were fixed, respectively, along the horizontal and vertical directions. The gradient model was constructed by extracting the fourth quadrant of a set of concentric ellipses with an aspect ratio of 1.5 between the major and minor axes. The mesh size of the unidirectional composites and the minimal mesh size of the gradient one were set as 1.25 μm. The structure and mechanical properties of the constituents in biological materials vary significantly among different species; in particular, the mechanical properties depend strongly on the hierarchical levels of materials and test conditions, such as the hydration states and strain rates [21,24,35]. As such, it is difficult to determine accurate values of the involved parameters for the modeling. Nonetheless, the global varying trend of the indentation behavior among the composites with distinct structures remains constant despite the uncertain values. Below we attempt to clarify the beneficial effects of the gradient structural orientations to create a protective role by defining a suit of appropriate parameters.

The individual layer thickness of the hard phase was set at 3 times as that of the soft phase, with values of 7.5 μm and 2.5 μm for the hard and soft phases, respectively, in the unidirectional composites and on the top surface of the gradient one; as such, the volume fractions of the two phases are 0.75 and 0.25, respectively. The Young's moduli were set as 70 GPa and 10 GPa for the hard and soft phases, respectively, giving the parameter k as 7. The Poisson's ratio was chosen as 0.3 for both constituents and an ideally tight bonding was defined between them. Two situations were analyzed by considering the constituents as perfectly linear elastic and elastic-plastic materials. For the latter case, the von Mises yield criterion was employed with the yield strengths of the hard and soft phases set respectively as 700 MPa and 100 MPa. Hypothetical attack, *e.g.*, caused by predatory biting, was simulated by applying an indentation load of 25 N that was uniformly distributed on the contact area equaling to the thickness of a dozen constituent layers, *i.e.*, 60 μm.

The indentation load-displacement curves and resultant contours of equivalent von Mises stress and strain energy density for linear elastic and elastic-plastic situations are presented in Figs. 7 and 8. In the composite where the structure and external force are commensurate, the applied stress is easily transferred into the interior along the longitudinal direction, yet is constrained within a narrow region transversely. The corresponding strain energy is concentrated over a small area beneath the indenter. As such, it is easy for the contact damage to initiate and develop inwards along the structural features. By comparison, the magnitudes of both stress and strain energy are lowered in the orthotropic composite. The stress is constrained within the reduced

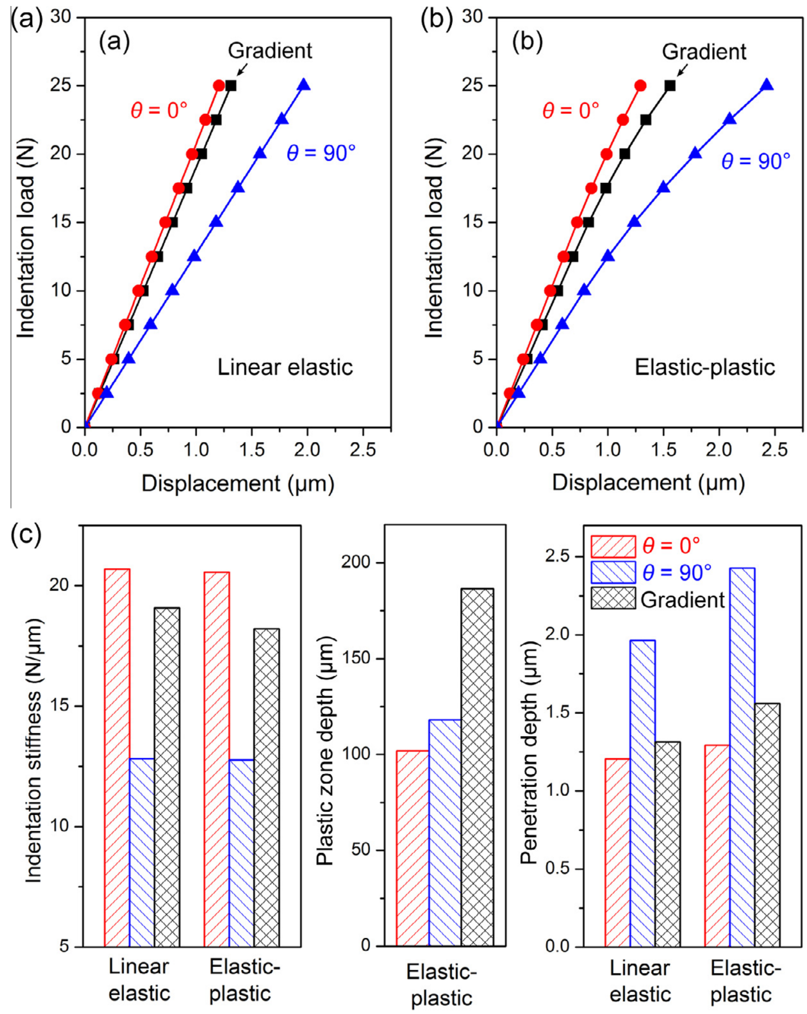

Fig. 7. Calculated indentation load-displacement curves for the composites with distinct structural orientations under linear elastic (a) and elastic-plastic (b) conditions under indentation based on a finite element simulation. (c) Comparison of the nominal indentation stiffness, the depth of plastic deformation zone and the penetration depth of the composites.

thickness as a result of the less smooth load transfer between different phases, such that the energy is more widely distributed. Nevertheless, the mechanical efficiency of the internal material may not be fully utilized for protection as the deformation zone continuously shrinks from the subsurface towards the interior.

In contrast, the indentation stress is distributed over a broader region with a low depth in the composite with varying structural orientation. The deformation zone expands asymmetrically with increasing distance from the loading site so that more material participates in accommodating the stress as it transfers inwards. The strain energy is also consumed by a larger area compared to the unidirectionally axial composite, while the energy concentration near the contact surface, especially in the soft phase, is alleviated compared to the orthotropic material. Indeed, the nominal indentation stiffness of the gradient composite, as represented by the slope of the near linear stage on the load-displacement curve, is comparable to that of the axial case loaded along the longitudinal direction; both are superior to the orthotropic material (Fig. 7c). The depth of the plastic deformation zone corresponding to a plastic strain of 0.1% is highest in the composite with the gradient structural orientation, signifying the ease of plastic deformation towards its interior which helps consume more mechanical energy. Additionally, the penetration depths, *i.e.*, the concavity of the contact surface, are respectively ~33% and ~35% lower than those of the orthotropic composite for the linear elastic and elastic-plastic situations. Therefore, the varying structural orientation can effectively contribute to improved contact damage resistance, thereby rendering the composite with an enhanced protective role.

5. Bioinspired design of orientation gradients

Natural gradients in structural orientations can provide a salient design motif to be mimicked in synthetic materials, particularly for the case of armor. Here, we outline the design strategy for such a bioinspired architecture in terms of the geometry of individual constituent layers. These layers are assumed to be tilted following an elliptical-shaped trajectory which is a basic mathematic model describing continuously varying orientation, as shown in Fig. 9. The major (transverse) and minor (longitudinal) axes of the ellipse are denoted as a and b, respectively. The orientation angle θ at depth h can then be expressed according to the slope of the tangent as:

$$\theta = \arctan \frac{ah}{b\sqrt{b^2 - h^2}}. \tag{13}$$

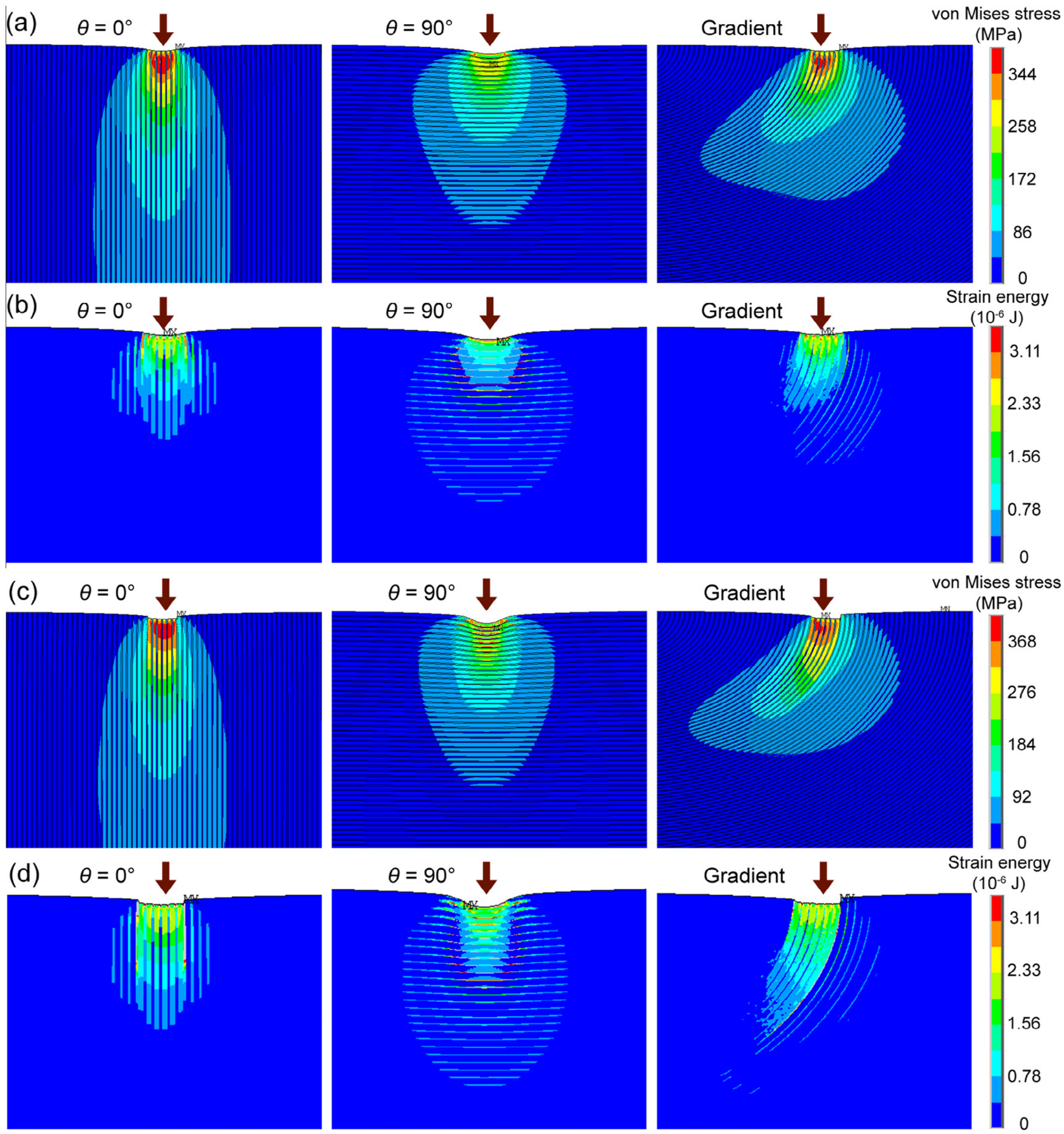

Fig. 8. Contours of the equivalent von Mises stress and strain energy density in the composites with distinct structural orientations under linear elastic (a, b) and elastic-plastic (c, d) conditions under indentation loading based on a finite element analysis simulation. The deformation zones under the indenter were magnified to assist in the comparison.

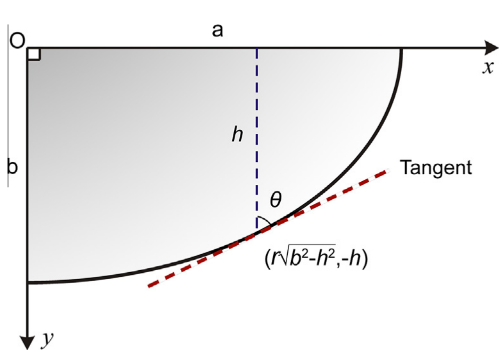

Fig. 9. Schematic illustration of the varying structural orientation in terms of the geometry of one individual constituent layer following elliptical-shaped trajectory.

By introducing the ellipse aspect ratio $r = a/b$ and normalizing h using b, Eq. (13) can be rearranged as:

$$\theta = \arctan\frac{rt}{\sqrt{1-t^2}}, \tag{14}$$

where $t = h/b$ ($0 \leqslant t \leqslant 1$). As shown in Fig. 10, the increasing trend of θ with the depth from the surface can be readily controlled by tuning r. The gradient becomes more gradual near the surface, yet much steeper towards the interior, as r decreases, and *vice versa*.

The local mechanical properties of the composite, *i.e.*, normalized stiffness, strength and fracture resistance, at relative depth t can then be obtained by incorporating Eq. (14) into Eqs. (4), (6) and (12). The involved parameters can be pre-designed by tuning the geometry and properties of the constituents, thus allowing deliberate control of the property gradients. As an example, the situation for a suit of parameters taken as $k = 10$, $V_A = 0.4$, $m = 5$, $n = 0.7$ and $r = 2$ are presented in Fig. 11. The ranges of the property gradients can be further designated by locating the structural features within different intervals of depth.

It is fairly challenging to attain both high strength/stiffness and good toughness within the same material as these properties tend to be mutually exclusive [54,64]. Although such conflicts are not subjugated in the present composite, as evidenced by the opposite varying trends (Fig. 11), a number of distinct advantages, *e.g.*, a stiff

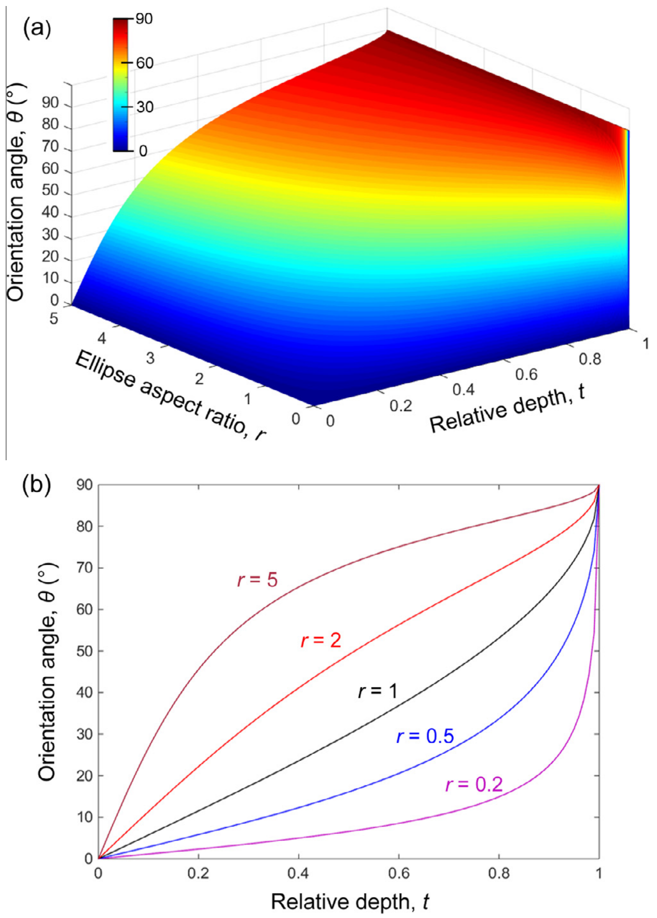

Fig. 10. (a) Dependences of the orientation angle θ on the ellipse aspect ratio r and relative depth t in the composite with gradient structural orientations. (b) Variations in θ as a function of t for representative cases of different r, ranging from 0.2 to 5.

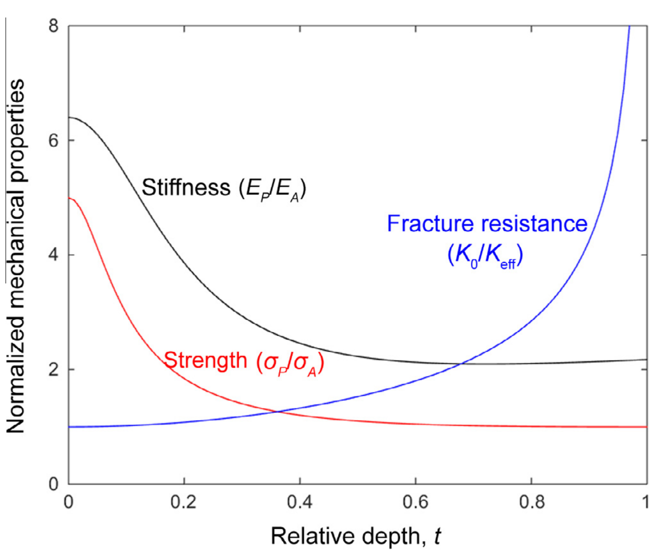

Fig. 11. Variations in normalized mechanical properties of stiffness E_P/E_A, strength σ_P/σ_A and fracture resistance K_0/K_{eff} as a function of relative depth t in the composite with representative parameters as $k = 10$, $V_A = 0.4$, $m = 5$, $n = 0.7$ and $r = 2$.

and wear-resistant surface, a compliant base and an increasing toughness towards the interior, are ingeniously combined though the varying structural orientations, leading to enhanced contact damage resistance without manipulation of local composition and/or microstructural dimensions. The naturally-occurring gradients are invariably the products of complex biological processes, *e.g.*, bio-mineralization, that are difficult to replicate in engineering design. Nonetheless, the underlying principle may be translated into synthetic materials through carefully controlling the fabrication parameters, such as the temperature gradient. In particular, the development of unique processing techniques that possess similar "bottom-up" sequences as in biological materials, *e.g.*, epitaxial deposition, freeze casting and additive manufacturing [65–70], offers more feasible approaches to control the structure of materials, thus making the bioinspired gradients in structural orientation increasingly practical for enhanced mechanical properties in structural materials.

6. Conclusions

With their hierarchical architectures incorporating gradients in composition, structure and orientation, biological systems have evolved optimized structures and properties under their ecological conditions and as such act as an inexhaustible source of inspiration for the development of high-performance synthetic materials, specifically functionally graded materials. Continuously varying structural orientations have been adopted by a variety of biological tissues and materials at multiple length-scales, where the directionality of the structure deviates from that of the external forces with increasing distance from the loading site. Such architectures offer functionally graded mechanical properties, *i.e.*, the local stiffness and strength that decrease monotonically from the surface towards the interior, with a fracture resistance that varies inversely due to enhanced extrinsic toughening from continuous crack deflection. This helps suppress the elastic/plastic deformation and damage near the surface of the material and accommodate the stress and dissipate mechanical energy towards its interior, making any cracking in the inward direction increasingly more difficult. As such, the contact damage resistance of materials is enhanced to provide greater protection to surface penetration. These merits are visualized and corroborated by numerical simulations of the indentation behavior of composites with distinct structural orientations. We believe that this design motif can be translated into synthetic materials by manipulating the structure in terms of the geometry of constituent layers. This study may therefore present new opportunities for developing high-performance FGMs with enhanced protection through the bioinspired design of gradients in structural orientation.

Acknowledgements

This work was supported by the Multidisciplinary University Research Initiative grant #AFOSR-FA9550-15-1-0009 from the Air Force Office of Scientific Research to the University of California Riverside, specifically through a subcontract to the University of California Berkeley (ZQL and ROR), and by the National Natural Science Foundation of China under grant numbers of 51501190 and 51331007 (ZQL, YKZ, DJ, ZYW and ZFZ). The authors would like to thank Prof. Marc A. Meyers for his helpful input to this study.

References

[1] M. Koizumi, M. Niino, Overview of FGM research in Japan, MRS Bull. 20 (1995) 19–21.
[2] M. Koizumi, FGM activities in Japan, Compos. Part B-Eng. 28 (1997) 1–4.
[3] A. Mortensen, S. Suresh, Functionally graded metals and metal-ceramic composites: part 1 processing, Inter. Mater. Rev. 40 (1995) 239–265.
[4] S. Suresh, A. Mortensen, Functionally graded metals and metal-ceramic composites: part 2 thermomechanical behavior, Int. Mater. Rev. 42 (1997) 85–116.

[5] A.E. Giannakopoulos, S. Suresh, M. Finot, M. Olsson, Elastoplastic analysis of thermal cycling: layered materials with compositional gradients, Acta Metall. Mater. 43 (1995) 1335–1354.
[6] S. Suresh, Graded materials for resistance to contact deformation and damage, Science 292 (2001) 2447–2451.
[7] D.C. Pender, N.P. Padture, A.E. Giannakopoulos, S. Suresh, Gradients in elastic modulus for improved contact-damage resistance. Part I: the silicon nitride-oxynitride glass system, Acta Mater. 49 (2001) 3255–3262.
[8] T.H. Fang, W.L. Li, N.R. Tao, K. Lu, Revealing extraordinary intrinsic tensile plasticity in gradient nano-grained copper, Science 331 (2011) 1587–1590.
[9] O. Jorgensen, A.E. Giannakopoulos, S. Suresh, Spherical indentation of composite laminates with controlled gradients in elastic anisotropy, Int. J. Solids Struct. 35 (1998) 5097–5113.
[10] A.R. Studart, Biological and bioinspired composites with spatially tunable heterogeneous architectures, Adv. Funct. Mater. 23 (2013) 4423–4436.
[11] A.R. Studart, R. Libanori, R.M. Erb, Functional gradients in biological composites, in: D. Ruiz-Molina, F. Novio, C. Roscini (Eds.), Bio- and Bioinspired Nanomaterials, Wiley-VCH, Weinheim, 2014.
[12] F. Nogata, H. Takahashi, Intelligent functionally graded material: bamboo, Compos. Eng. 5 (1995) 743–751.
[13] M.K. Habibi, A.T. Samaei, B. Gheshlaghi, J. Lu, Y. Lu, Asymmetric flexural behavior from bamboo's functionally graded hierarchical structure: underlying mechanisms, Acta Biomater. 16 (2015) 178–186.
[14] B.J.F. Bruet, J. Song, M.C. Boyce, C. Ortiz, Materials design principles of ancient fish armor, Nat. Mater. 7 (2008) 748–756.
[15] W. Yang, I.H. Chen, B. Gludovatz, E.A. Zimmermann, R.O. Ritchie, M.A. Meyers, Natural flexible dermal armor, Adv. Mater. 25 (2013) 31–48.
[16] W. Yang, V.R. Sherman, B. Gludovatz, M. Mackey, E.A. Zimmermann, E.H. Chang, E. Schaible, Z. Qin, M.J. Buehler, R.O. Ritchie, M.A. Meyers, Protective role of *Arapaima gigas* fish scales: structure and mechanical behavior, Acta Biomater. 10 (2014) 3599–3614.
[17] R. Menig, M.H. Meyers, M.A. Meyers, K.S. Vecchio, Quasi-static and dynamic mechanical response of *Haliotis rufescens* (abalone) shells, Acta Mater. 48 (2000) 2383–2398.
[18] D. Jiao, Z.Q. Liu, Z.J. Zhang, Z.F. Zhang, Intrinsic hierarchical structural imperfections in a natural ceramic of bivalve shell with distinctly graded properties, Sci. Rep. 5 (2015) 12418.
[19] C.Y. Sun, P.-Y. Chen, Structural design and mechanical behavior of alligator (*Alligator mississippiensis*) osteoderms, Acta Biomater. 9 (2013) 9049–9064.
[20] H.P. Lian, D.R. Tan, Study on bimetallic bronze swords in ancient China, Sci. Conserv. Archaeol. 14 (2002) 319–334.
[21] M.A. Meyers, J. Mckittrick, P.-Y. Chen, Structural biological materials: critical mechanics-materials connections, Science 339 (2013) 773–779.
[22] P. Fratzl, R. Weinkamer, Nature's hierarchical materials, Prog. Mater Sci. 52 (2007) 1263–1334.
[23] E.A. Zimmermann, R.O. Ritchie, Bone as a structural material, Adv. Healthcare Mater. 4 (2015) 1287–1304.
[24] M.A. Meyers, P.-Y. Chen, A.Y.M. Lin, Y. Seki, Biological materials: structure and mechanical properties, Prog. Mater Sci. 53 (2008) 1–206.
[25] J. Song, C. Ortiz, M.C. Boyce, Threat-protection mechanics of an armored fish, J. Mech. Behav. Biomed. Mater. 4 (2011) 699–712.
[26] L. Tombolato, E.E. Novitskaya, P.-Y. Chen, F.A. Sheppard, J. McKittrick, Microstructure, elastic properties and deformation mechanisms of horn keratin, Acta Biomater. 6 (2010) 319–330.
[27] D. Konjevic, U. Kierdorf, L. Manojlovic, K. Severin, Z. Janicki, A. Slavica, B. Reindl, I. Pivac, The spectrum of tusk pathology in wild boar (*Sus scrofa* L.) from Croatia, Vet. Arhiv. 76 (2006) S91–S100.
[28] D. Raabe, A. Al-Sawalmih, S.B. Yi, H. Fabritius, Preferred crystallographic texture of α-chitin as a microscopic and macroscopic design principle of the exoskeleton of the lobster *Homarus americanus*, Acta Biomater. 3 (2007) 882–895.
[29] P.-Y. Chen, A.Y.M. Lin, J. McKittrick, M.A. Meyers, Structure and mechanical properties of crab exoskeletons, Acta Biomater. 4 (2008) 587–596.
[30] Z.-L. Zhao, T. Shu, X.-Q. Feng, Study of biomechanical, anatomical, and physiological properties of scorpion stingers for developing biomimetic materials, Mater. Sci. Eng., C 58 (2016) 1112–1121.
[31] Y. Politi, M. Priewasser, E. Pippel, P. Zaslansky, J. Hartmann, S. Siegel, C. Li, F.G. Barth, P. Fratzl, A spider's fang: how to design an injection needle using chitin-based composite material, Adv. Funct. Mater. 22 (2012) 2519–2528.
[32] B. Bar-On, F.G. Barth, P. Fratzl, Y. Politi, Multiscale structural gradients enhance the biomechanical functionality of the spider fang, Nat. Commun. 5 (2014) 3894.
[33] J.H. Waite, H.C. Lichtenegger, G.D. Stucky, P. Hansma, Exploring molecular and mechanical gradients in structural bioscaffolds, Biochemistry 43 (2004) 7653–7662.
[34] M.G. Pontin, D.N. Moses, J.H. Waite, F.W. Zok, A nonmineralized approach to abrasion-resistant biomaterials, Proc. Natl. Acad. Sci. U.S.A. 104 (2007) 13559–13564.
[35] B. Wang, W. Yang, J. McKittrick, M.A. Meyers, Keratin: structure, mechanical properties, occurrence in biological organisms, and efforts at bioinspiration, Prog. Mater Sci. 76 (2016) 229–318.
[36] Z.Q. Liu, D. Jiao, Z.Y. Weng, Z.F. Zhang, Structure and mechanical behaviors of armored pangolin scales and the effects of hydration and orientation, J. Mech. Behav. Biomed. Mater. 56 (2016) 165–174.
[37] S. Bentov, P. Zaslansky, A. Al-Sawalmih, A. Masic, P. Fratzl, A. Sagi, A. Berman, B. Aichmayer, Enamel-like apatite crown covering amorphous mineral in a crayfish mandible, Nat. Commun. 3 (2012) 839.
[38] P. Zaslansky, S. Zabler, P. Fratzl, 3D variations in human crown dentin tubule orientation: a phase-contrast microtomography study, Dent. Mater. 26 (2010) e1–e10.
[39] J.D. Currey, K. Brear, P. Zioupos, Dependence of mechanical properties on fibre angle in narwhal tusk, a highly oriented biological composite, J. Biomech. 27 (1994) 885–897.
[40] D.F.G. Poole, A.W. Brooks, The arrangement of crystallites in enamel prisms, Arch. Oral Biol. 5 (1961) IN5–26.
[41] A. Boyde, The structure and development of mammalian enamel (Ph.D. thesis), University of London, London, 1964.
[42] S.F. Ang, E.L. Bortel, M.V. Swain, A. Klocke, G.A. Schneider, Size-dependent elastic/inelastic behavior of enamel over millimeter and nanometer length scales, Biomaterials 31 (2010) 1955–1963.
[43] Z.H. Xie, E.K. Mahoney, N.M. Kilpatrick, M.V. Swain, M. Hoffman, On the structure-property relationship of sound and hypomineralized enamel, Acta Biomater. 3 (2007) 865–872.
[44] F.T. Wallenberger, N.E. Weston, Natural Fibers, Plastics and Composites, Springer Science & Business Media, New York, 2004.
[45] S.E. Naleway, M.M. Porter, J. McKittrick, M.A. Meyers, Structural design elements in biological materials: application to bioinspiration, Adv. Mater. 27 (2015) 5455–5476.
[46] L.J. Wolfram, Human hair: a unique physicochemical composite, J. Am. Acad. Dermatol. 48 (2003) S106–S114.
[47] R.M. Jones, Mechanics of Composite Materials, 2nd ed., Taylor & Francis, Philadelphia, 1999.
[48] Z.Q. Liu, D. Jiao, M.A. Meyers, Z.F. Zhang, Structure and mechanical properties of naturally occurring lightweight foam-filled cylinder - the peacock's tail coverts shaft and its components, Acta Biomater. 17 (2015) 137–151.
[49] V.D. Azzi, S.W. Tsai, Anisotropic strength of composites, Exp. Mech. 5 (1965) 283–288.
[50] R. Hill, Theory of mechanical properties of fibre-strengthened materials: I. Elastic behavior, J. Mech. Phys. Solids 12 (1964) 199–212.
[51] S.P. Timoshenko, J.N. Goodier, Theory of Elasticity, 3rd ed., Tsinghua University Press, Beijing, 2004.
[52] S.W. Tsai, Theory of Composites Design, Think Composites, Dayton, 1992.
[53] M.E. Launey, R.O. Ritchie, On the fracture toughness of advanced materials, Adv. Mater. 21 (2009) 2103–2110.
[54] R.O. Ritchie, In pursuit of damage tolerance in engineering and biological materials, MRS Bull. 39 (2014) 880–890.
[55] R.O. Ritchie, M.J. Buehler, P. Hansma, Plasticity and toughness in bone, Phys. Today 62 (2009) 41–47.
[56] K.J. Koester, J.W. Ager, R.O. Ritchie, The true toughness of human cortical bone measured with realistically short cracks, Nat. Mater. 7 (2008) 672–677.
[57] B.R. Lawn, Fracture of Brittle Solids, 2nd ed., Cambridge University Press, New York, 1993.
[58] L.P. Pook, The effect of crack angle on fracture toughness, Eng. Fract. Mech. 3 (1971) 205–218.
[59] J.J. Petrovic, M.J. Mendiratta, Mixed-mode fracture from controlled surface flaws in hot-pressed Si_3N_4, J. Am. Ceram. Soc. 59 (1976) 163–167.
[60] S. Suresh, Crack deflection: implications for the growth of long and short fatigue cracks, Metall. Trans. A 14 (1983) 2375–2385.
[61] Y. Murakami, Analysis of stress intensity factors of modes I, II and III for inclined surface cracks of arbitrary shape, Eng. Fract. Mech. 22 (1985) 101–114.
[62] R.O. Ritchie, J.H. Kinney, J.J. Kruzic, R.K. Nalla, A fracture mechanics and mechanistic approach to the failure of cortical bone, Fatigue Fract. Eng. Mater. Struct. 28 (2005) 345–371.
[63] D. Bajaj, D.D. Arola, On the *R*-curve behavior of human tooth enamel, Biomaterials 30 (2009) 4037–4046.
[64] R.O. Ritchie, The conflicts between strength and toughness, Nat. Mater. 10 (2011) 817–822.
[65] U.G.K. Wegst, H. Bai, E. Saiz, A.P. Tomsia, R.O. Ritchie, Bioinspired structural materials, Nat. Mater. 14 (2015) 23–36.
[66] E. Munch, M.E. Launey, D.H. Alsem, E. Saiz, A.P. Tomsia, R.O. Ritchie, Tough, bio-inspired hybrid materials, Science 322 (2008) 1516–1520.
[67] L.S. Dimas, G.H. Bratzel, I. Eylon, M.J. Buehler, Tough composites inspired by mineralized natural materials: computation, 3D printing, and testing, Adv. Funct. Mater. 23 (2013) 4629–4638.
[68] J.A. Lewis, Colloidal processing of ceramics, J. Am. Ceram. Soc. 83 (2000) 2341–2359.
[69] L.J. Bonderer, A.R. Studart, L.J. Gauckler, Bioinspired design and assembly of platelet reinforced polymer films, Science 319 (2008) 1069–1073.
[70] J.J. Martin, B.E. Fiore, R.M. Erb, Designing bioinspired composite reinforcement architectures via 3D magnetic printing, Nat. Commun. 6 (2015) 8641.